Reflection Analysis of FDTD Boundary Conditions—Part I: Time-Space Absorbing Boundaries

Deane T. Prescott, *Member, IEEE,* and Nicholas V. Shuley, *Member, IEEE*

***Abstract*—Time-space absorbing-boundary conditions (ABC's) are employed to truncate finite-difference time-domain (FDTD) computational domains and are predominantly used because of their simplicity. Their implementation requires only the calculation of a boundary-field value as a function of the local fields and their recent time history. A general method is described, which enables highly accurate calculation of the reflection properties of these boundary conditions for plane-wave incidence. A number of commonly used time-space ABC's are studied, and the technique is verified by way of FDTD simulation. It is demonstrated that the performance of time-space ABC's is substantially degraded by the influence of the finite-mesh discretizations. A technique is described, which enables these discretization inaccuracies to be overcome by correctly choosing the relevant ABC weighting parameters, thus enabling the various boundary conditions to perform precisely as desired. Solutions for these weighting parameters are provided for a number of common boundary conditions such that their absorption characteristics may be precisely configured to suit any level of mesh discretization. As a consequence, a performance equivalence is established amongst all time-space ABC's of the same order.**

***Index Terms*— Absorbing boundary conditions, FDTD, time domain.**

I. Introduction

ABSORBING-BOUNDARY conditions (ABC's) are one of the most critical elements of finite-difference time-domain (FDTD) analyses. Used to truncate the computational domain, the ability of an ABC to absorb waves traveling outwardly from an FDTD mesh, not only affects the accuracy of the analysis, but also governs the size of the computational domain and, as a result, the duration of computation.

In this paper, time-space-type ABC's are studied. These are ABC's where the field component on the mesh boundary at time $t = n$ is calculated as a function of the local field components, both on the boundary and within the FDTD lattice, and their recent time history, $t = n - i$, where $i = 0, 1, 2 \cdots$.

Many studies have been undertaken in the past concerning time-space ABC's. These have included the creation of different ABC's and their variants [1]–[4], studying their absorbing abilities [5], [6], and methods for their improvement [7]–[9]. The effects that the finite discretization has upon ABC's and the absorption characteristics for coarse and fine FDTD meshes has also been studied by Railton and Daniel [10]. The objective of this paper is to demonstrate that the reflection characteristics of these boundaries can be accurately predicted without the need for FDTD simulation. It will then be shown that the mesh discretization can be overcome as a limiting factor in the design of time-space ABC's.

Firstly, some definitions that apply to this study of time-space ABC's will be provided. These include the performance function, the optimum performance, and the *order* by which these ABC's will be classified. A method for evaluating the performance of these ABC's given plane-wave incidence will be presented, which will be validated using three ABC's appearing very frequently in the literature. These are the second-order ABC of Trefethen and Halpern [2], box-scheme discretization of the second-order Higdon ABC [3], and second-order modified Liao ABC [11]. Finally, it will be shown that given the correct choice of parameters (as a function of the mesh resolution), each of these boundary conditions can be designed to perform optimally (in the sense that they are perfectly absorbing at specified angles of incidence).

For simplicity, the analyses will be presented for two-dimensional (2-D) free-space on the x–z plane. (the y-direction is not used to avoid confusion between the FDTD y-directed nodal index j, and the numerical $j = \sqrt{-1}$.) The theory and methods presented here are applicable to mesh truncation in three-dimensional (3-D) space and dispersive media.

II. Definitions

Performance: The ability for an ABC to absorb will be measured by the amount of numerical reflection as a function of the angle of incidence upon the mesh boundary. If free-space and monochromatic excitation are assumed, then choosing a mesh discretization size $\lambda/\Delta z$ (wavelength/mesh cell size) to set the level of accuracy for the FDTD simulation will also specify the frequency, ω, of the incident wave.

Incidence Angle: The angle of incidence, θ, of a wave upon a boundary in an FDTD simulation is defined as

$$\theta = \tan^{-1}\left(\frac{k_x}{k_z}\right) \tag{1}$$

Manuscript received October 17, 1995; revised April 25, 1997.

D. T. Prescott was with the Department of Electrical and Computer Engineering, The University of Queensland, Qld., Q4072, Australia. He is now with the Australian Defense Science and Technology Organization (DSTO), Salisbury, S.A. 5108, Australia.

N. V. Shuley is with the Department of Electrical and Computer Engineering, The University of Queensland, Qld., Q4072, Australia.

Publisher Item Identifier S 0018-9480(97)05371-4.

where k_z and k_x are the normal and tangential components of the numerical wavenumber. These are related to the frequency by the FDTD dispersion relation [12].

Order (N): The order of an ABC is defined as the number of zeros which can be achieved in the reflection function of an ABC. The reflection function describes the performance of an ABC as a function of the incidence angle.

Optimum Performance: Occurs when the reflection function has zeros at the desired angles of incidence (ϕ_i), and is a minimum for all other incident angles θ. This can be described approximately for time-space ABC's of order N as [13]

$$|R_{\rm opt}| = \prod_{i=1}^{N} \frac{\cos(\phi_i) - \cos(\theta)}{\cos(\phi_i) + \cos(\theta)}. \tag{2}$$

III. Reflection Analysis by Numerical Formulation

A number of methods for calculating the reflection resulting from an ABC have been given in the literature. The amplitude of the reflection has been previously calculated from the differential equations from which the boundary conditions are derived [11], [14]. Unfortunately, these methods neglect the errors resulting from the discretization. Other authors have calculated the reflection from the discretized equations by substituting into them, expressions for the incident field as a function of space and time [8]. Again, this is not entirely accurate as it neglects the numerical dispersion inherent in the FDTD algorithm [15]. Thus, to calculate the reflection from the ABC's, it is suggested that one follows the method where the reflection from the ABC's is calculated by substituting directly into the discretized FDTD equations, expressions for the incident fields, which include the effects of the numerical dispersion. This will be referred to as the *formulation* method, and does not involve any actual FDTD simulation.

A general form for the time-space ABC is defined, where the boundary-field component, $E^0(0,0)$, is located at position $x = 0, z = 0$, and is required at time $t = 0$. The ABC is calculated as a weighted sum of the local field values and their time history

$$E^0(0,0) = \sum_{n=n_{\min}}^{0} \sum_{i=x_{\min}}^{x_{\max}} \sum_{k=0}^{z_{\max}} a(n,i,k) E^n(i,k), \qquad n \neq i \neq k = 0 \tag{3}$$

where $n_{\min}$, $x_{\min}$, $x_{\max}$, and $z_{\max}$ define the maximum and minimum indexes of the local time-space domain from which the boundary field is calculated. The weighting elements, $a(n,i,k)$, are defined individually for each ABC.

Now an incident plane-wave traveling to the left ($-z$-direction) can be defined as

$$E^n_{\rm inc}(i,k) = E_0 e^{j(\omega n\Delta t - k_x i\Delta x + k_z k\Delta z)} \tag{4}$$

where k is the spatial position index in the normal (to the boundary) direction, i is the spatial position in the tangential direction, n is the time index, and k_x and k_z are the tangential and normal numerically calculated wavenumbers (numerically calculated, implying that they are related to each other by the FDTD dispersion relation [12]).

When this wave makes contact with the absorbing boundary, it produces a total field consisting of incident- and reflected-wave components

$$\begin{aligned} E^n(i,k) &= E^n_{\rm inc}(i,k) + R_{\rm ABC}\, E^n_{\rm ref}(i,k) \\ &= E_0 e^{j(\omega n\Delta t - k_x i\Delta x + k_z k\Delta z)} \\ &\quad + R_{\rm ABC}\, E_0 e^{j(\omega n\Delta t - k_x i\Delta x - k_z k\Delta z)} \end{aligned} \tag{5}$$

where $R_{\rm ABC}$ is the reflection coefficient. This formulation for the $E^n(i,k)$-field components can then be substituted into (3) to form a relationship between the ABC reflection coefficient and the ABC weighting functions. Thus

$$\begin{aligned} &E_0 + R_{\rm ABC}\, E_0 \\ &\quad = \sum_{n=n_{\min}}^{0} \sum_{i=x_{\min}}^{x_{\max}} \sum_{k=0}^{z_{\max}} \Big(a(n,i,k) E_0 e^{j(\omega n\Delta t - k_x i\Delta x + k_z k\Delta z)} \\ &\qquad + R_{\rm ABC}\, a(n,i,k) E_0 e^{j(\omega n\Delta t - k_x i\Delta x - k_z k\Delta z)} \Big). \end{aligned} \tag{6}$$

If the right-hand side (RHS) of (6) is separated into two summations representing the incident and reflected fields, one can then solve for the reflection coefficient $R_{\rm ABC}$ shown in (7) at the bottom of the page. Given the frequency and angle of incidence, one can calculate the wavenumbers k_x and k_z, and thus, the reflection from the time-space ABC.

For example, an ABC may be defined with the following discrete equations:

$$E^n(0,0) = E^{n-1}(0,1) + \gamma(E^{n-1}(0,0) - E^n(0,1)) \tag{8}$$

where

$$\gamma = \frac{\Delta z - c\Delta t}{\Delta z + c\Delta t}. \tag{9}$$

Here, $a(0,0,1) = -\gamma$, $a(-1,0,0) = \gamma$, and $a(-1,0,1) = 1$ are constants, which determine the nature of the boundary condition. In this case, the first-order Mur absorbing boundary [1] is chosen. One can also find the corresponding equation for the reflection coefficient as

$$R_{\rm ABC} = -\frac{1 - e^{-j\omega\Delta t + jk_z\Delta z} - \gamma e^{-j\omega\Delta t} + \gamma e^{+jk_z\Delta z}}{1 - e^{-j\omega\Delta t - jk_z\Delta z} - \gamma e^{-j\omega\Delta t} + \gamma e^{-jk_z\Delta z}}. \tag{10}$$

$$R_{\rm ABC} = -\frac{1 - \sum_{n=n_{\min}}^{0} \sum_{i=x_{\min}}^{x_{\max}} \sum_{k=0}^{z_{\max}} a(n,i,k) e^{j(\omega n\Delta t - k_x i\Delta x + k_z k\Delta z)}}{1 - \sum_{n=n_{\min}}^{0} \sum_{i=x_{\min}}^{x_{\max}} \sum_{k=0}^{z_{\max}} a(n,i,k) e^{j(\omega n\Delta t - k_x i\Delta x - k_z k\Delta z)}} \tag{7}$$

IV. Reflection Analysis by FDTD Simulation

The accuracy of the reflection-calculation technique presented in the previous section, will be demonstrated with results achieved by using FDTD simulation.

The FDTD reflection analysis was performed using a novel quasi-2-D FDTD mesh designed to simulate TM^y-wave transmission within 2-D space (x–z plane, E_y, H_x, H_z components only). A monochromatic wave is launched at an ABC boundary, which terminates the mesh in the z-direction, and the magnitude of the reflected wave is recorded.

The simulation is performed at a single frequency, for a given angle of incidence. Because the calculation of an ABC is uniform across the full length of a boundary, the wavefront, which reflects from an ABC, must now have the same tangential wavenumber k_x as the incident wave (angle of reflection equals angle of incidence). A monochromatic excitation is being used, which implies that all fields within the FDTD mesh must have the same tangential wavenumber. This fact can be used to considerably reduce the size of the FDTD mesh without loss of accuracy. This is achieved by removing the transverse direction, thus creating a quasi-2-D FDTD mesh.

The FDTD simulation is performed using complex numbers to represent the nodal-field values, this aids in calculating the transverse differences and in extracting reflection data. In reality, only a one-dimensional (1-D) mesh is created which contains all three field components required in the 2-D mesh (see Fig. 1). The existence of the second dimension, in this case, the x-direction, is taken into account by implicitly calculating the tangential spatial differences in the FDTD equations. This is possible since all fields within the mesh must have the same wavenumber in the x-direction. Consider, for example, the FDTD equation for the E_y-field component

$$E_y^{n+1}(i,k) = E_y^n(i,k) + \frac{\Delta t}{\epsilon}\left[\frac{H_x^{n+\frac{1}{2}}\left(i,k+\frac{1}{2}\right) - H_x^{n+\frac{1}{2}}\left(i,k-\frac{1}{2}\right)}{\Delta z}\right] - \frac{\Delta t}{\epsilon}\left[\frac{H_z^{n+\frac{1}{2}}\left(i+\frac{1}{2},k\right) - H_z^{n+\frac{1}{2}}\left(i-\frac{1}{2},k\right)}{\Delta x}\right]. \quad (11)$$

The term which contains the spatial difference in the tangential to the boundary direction is

$$\frac{H_z^{n+\frac{1}{2}}\left(i+\frac{1}{2},k\right) - H_z^{n+\frac{1}{2}}\left(i-\frac{1}{2},k\right)}{\Delta x} \quad (12)$$

but since the tangential component of the wavenumber is being enforced, then $H_z^{n+\frac{1}{2}}(i+\frac{1}{2},k) = H_z^{n+\frac{1}{2}}(i-\frac{1}{2},k)e^{-jk_x\Delta x}$. Making this substitution into (11), the implicitly differenced form of the FDTD equation for the E_y component becomes

$$E_y^{n+1}(i,k) = E_y^n(i,k) + \frac{\Delta t}{\epsilon}\left[\frac{H_x^{n+\frac{1}{2}}\left(i,k+\frac{1}{2}\right) - H_x^{n+\frac{1}{2}}\left(i,k-\frac{1}{2}\right)}{\Delta z}\right] + \frac{\Delta t}{\epsilon}H_z^{n+\frac{1}{2}}\left(i-\frac{1}{2},k\right)\left[\frac{1-e^{-jk_x\Delta x}}{\Delta x}\right]. \quad (13)$$

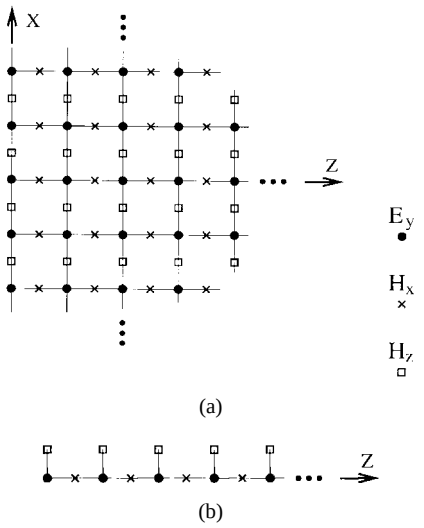

Fig. 1. Positioning of the field components required for the implementation of: (a) the normal 2-D FDTD mesh and (b) the quasi-2-D FDTD mesh.

The reflection from an ABC can now be accurately calculated for a given angle of incidence without the need for a large 2-D FDTD mesh, as the transverse x-direction is now implicitly included into the formulation. The possibility of interference from ABC's placed along the boundaries at each of the extremities of a 2-D FDTD mesh in the x-direction has also been removed.

For comparison of the reflection-calculation technique, the FDTD simulator described above has been applied to the reflection analysis of three different ABC's, which are: 1) the generalized second-order ABC of Trefethen and Halpern (formulation as described by Blaschak and Kriegsmann [5, p. 118]); 2) the second-order Higdon ABC using the box-scheme discretization (formulation as described by Bi, Wu, and Litva [16, p. 776]); and 3) the second-order modified Liao ABC [11, p. 538]. Each of these ABC's will be designed and analyzed for two different cases where the designated angles of complete absorption are: a) $\phi_1 = \phi_2 = 0°$ and b) $\phi_1 = 5°$ and $\phi_2 = 30°$. The weightings required to implement these ABC's will be provided; however, the reader is referred to the cited publications for a detailed description of their derivation.

Trefethen and Halpern's Second-Order ABC:

The weightings required to implement this ABC are as follows, all other weightings are set to zero:

$$\begin{aligned} a(-1,1,0) &= c_3 \\ a(-1,1,1) &= c_3 \\ a(-2,0,0) &= c_1 + c_2 \\ a(0,0,1) &= c_1 + c_2 \\ a(-1,0,0) &= -2c_2 - 2c_3 \\ a(-1,0,1) &= -2c_2 - 2c_3 \\ a(-2,0,1) &= -1 \\ a(-1,-1,0) &= c_3 \\ a(-1,-1,1) &= c_3 \end{aligned} \quad (14)$$

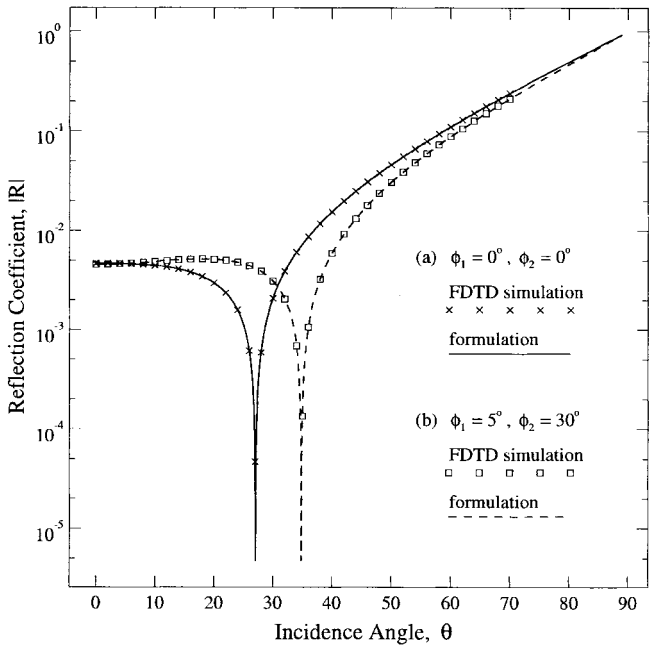

Fig. 2. The reflection function for the second-order Trefethen and Halpern ABC, calculated by FDTD simulation and numerical formulation $\lambda/\Delta z = 20$. Designated angles of complete absorption are: (a) $\phi_1 = \phi_2 = 0^\circ$ and (b) $\phi_1 = 5^\circ$ and $\phi_2 = 30^\circ$.

where

$$c_1 = \frac{c\Delta t}{p_0\Delta z + c\Delta t}$$
$$c_2 = -\frac{p_0\Delta z}{p_0\Delta z + c\Delta t}$$
$$c_3 = -\frac{p_2\Delta z}{p_0\Delta z + c\Delta t}\frac{c^2\Delta t^2}{\Delta x^2} \tag{15}$$

and

$$p_0 = \frac{\cos\phi_1\cos\phi_2 + 1}{\cos\phi_1 + \cos\phi_2}$$
$$p_2 = \frac{-1}{\cos\phi_1 + \cos\phi_2}. \tag{16}$$

The reflection function has been obtained using both the FDTD simulation and the numerical calculation procedure, described previously for two separate configurations of the ABC with the variables p_0 and p_2 (16), chosen such that the theoretical angles of complete absorption are: a) $\phi_1 = \phi_2 = 0^\circ$ and b) $\phi_1 = 5^\circ$ and $\phi_2 = 30^\circ$. It should be noted that this ABC is equivalent to the well-known second-order Mur ABC [1] for the case where $\phi_1 = \phi_2 = 0^\circ$.

The results from these calculations are provided in Fig. 2. As can be seen from these results, the calculation procedure has been extremely accurate in predicting the reflection function of the ABC. A number of properties of this boundary condition can also be observed. Firstly, the most obvious feature of these reflection functions is that the zeros do not appear in the positions as given by the choice of p_0 and p_2. In fact, only one zero appears in each reflection function where two should be seen. This occurs as a result of discretizing the differential equations which define the ABC [5], [10]. It can also be seen that as the incident angle is decreased below these zeros, the amount of reflection increases rapidly to quite high values, i.e., $\approx 10^{-2}$. Above these zeros, one can see a trend which is common to time-space ABC's, where the reflection function increases monotonically toward 1 at 90°.

Higdon's Second-Order ABC:

The weightings required to implement the box scheme discretization of Higdon's second-order ABC are as follows, with all other weightings being zero:

$$\begin{aligned} a(-1,0,0) &= \gamma_1 + \gamma_2 \\ a(-2,0,0) &= -\gamma_1\gamma_2 \\ a(0,0,1) &= -\gamma_1 - \gamma_2 \\ a(-1,0,1) &= 2 + 2\gamma_1\gamma_2 \\ a(-2,0,1) &= -\gamma_1 - \gamma_2 \\ a(0,0,2) &= -\gamma_1\gamma_2 \\ a(-1,0,2) &= \gamma_1 + \gamma_2 \\ a(-2,0,2) &= -1 \end{aligned} \tag{17}$$

where

$$\gamma_1 = \frac{\cos\phi_1\Delta z - c\Delta t}{\cos\phi_1\Delta z + c\Delta t}$$
$$\gamma_2 = \frac{\cos\phi_2\Delta z - c\Delta t}{\cos\phi_2\Delta z + c\Delta t}. \tag{18}$$

The reflection function has been obtained for this ABC using both the FDTD simulation and the numerical formulation procedure for two configurations of the Higdon ABC with the variables γ_1 and γ_2 (18) chosen, such that the theoretical angles of complete absorption are: a) $\phi_1 = \phi_2 = 0^\circ$ and b) $\phi_1 = 5^\circ$ and $\phi_2 = 30^\circ$.

Fig. 3 displays the results of these simulations. As can be seen from these results, the calculation procedure has again been extremely accurate in predicting the reflection function of the ABC. One can see that there is a slight discrepancy in the results where the reflection is less than $\approx 10^{-5}$. This is acceptable since numerical error will occur in the FDTD simulation owing to accumulating computational roundoff and the oscillatory nature of monochromatic FDTD simulations [17]. A much-improved performance (greater than one order) is obtained for this ABC over that achieved by the second-order Trefethen and Halpern ABC (see Fig. 2). Once again, the zeros are not exactly at the positions where they have been designed to be; however, their displacement is not too unacceptable.

The Second-Order Modified Liao ABC:

The Liao ABC [4] is a time-space extrapolation boundary condition based upon a knowledge of the incident wave. The formulation uses the fact that a wave normally incident upon a boundary, traveling at the speed of light, will travel a distance of $c\Delta t$ toward the boundary during one FDTD time step, where c is the speed of light. The Liao absorbing-boundary condition is then constructed as a linear time-space extrapolation of the fields at the $lc\Delta t$ points in space previous to the boundary at time $t = n - l\Delta t$ l integer. Because the points $lc\Delta t$ may not coincide with the nodes of the

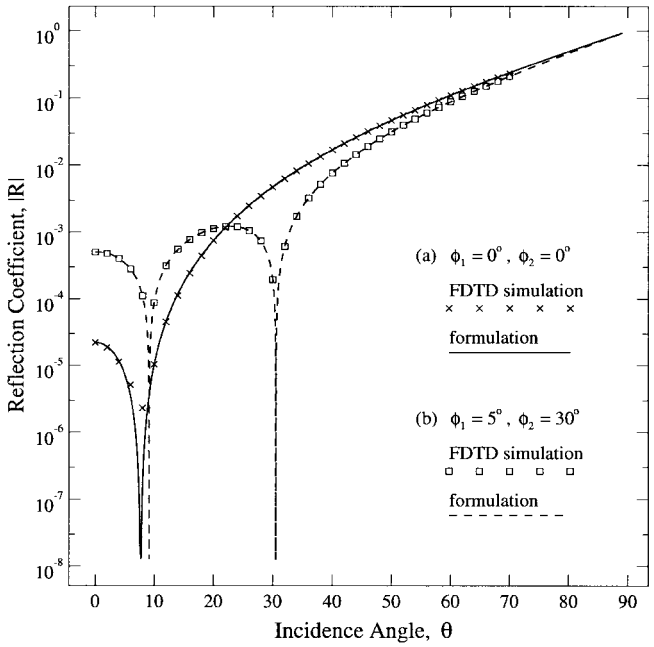

Fig. 3. The reflection function for the second-order Higdon ABC, calculated by FDTD simulation and numerical formulation $\lambda/\Delta z = 20$. Designated angles of complete absorption are: (a) $\phi_1 = \phi_2 = 0^\circ$ and (b) $\phi_1 = 5^\circ$ and $\phi_2 = 30^\circ$.

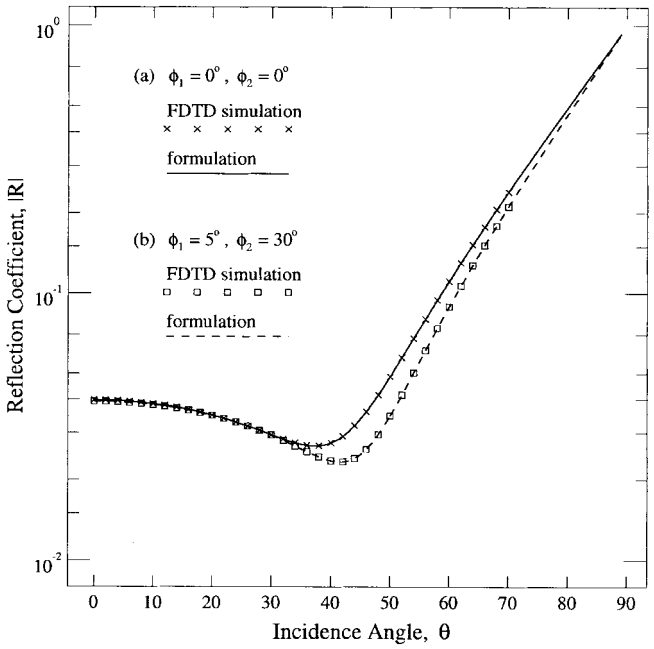

Fig. 4. The reflection function for the second-order modified Liao ABC. Calculated by FDTD simulation and numerical formulation, $\lambda/\Delta z = 20$. Designated angles of complete absorption are: (a) $\phi_1 = \phi_2 = 0^\circ$ and (b) $\phi_1 = 5^\circ$ and $\phi_2 = 30^\circ$.

FDTD mesh, it is necessary to use an interpolation scheme to implement this boundary condition [11].

The modified Liao ABC differs from the standard Liao ABC in that it is able to be tuned for absorption at desired angles of incidence. The weightings required for the modified Liao's second-order ABC resulting from the use of quadratic

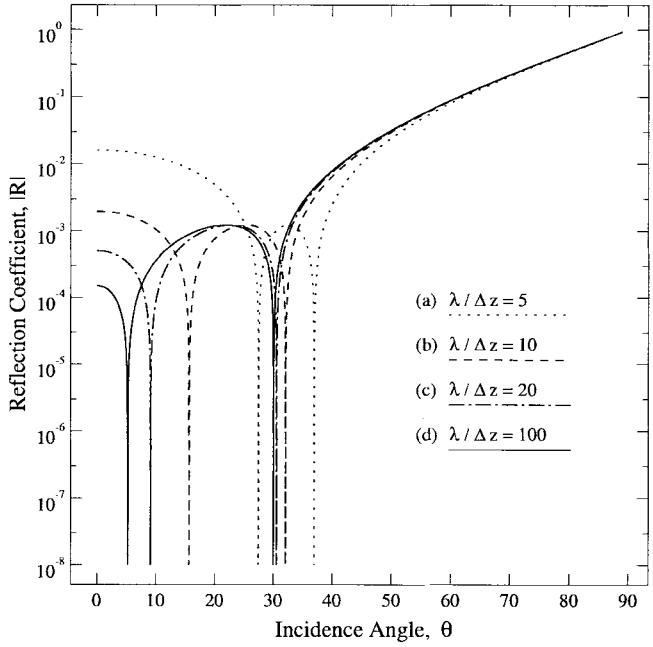

Fig. 5. The reflection function for the second-order Higdon ABC for different mesh discretizations. The designated angles of complete absorption for the ABC are $\phi_1 = 5^\circ$ and $\phi_2 = 30^\circ$. The mesh discretization ratios are: (a) $\lambda/\Delta z = 5$, (b) $\lambda/\Delta z = 10$, (c) $\lambda/\Delta z = 20$, and (d) $\lambda/\Delta z = 100$.

interpolation are as follows:

$$
\begin{aligned}
a(-1,0,0) &= \frac{c_1^2 + c_2^2 - 3c_1 - 3c_2 + 4}{2} \\
a(-1,0,1) &= \frac{-2c_1^2 - 2c_2^2 + 4c_1 + 4c_2}{2} \\
a(-1,0,2) &= \frac{c_1^2 + c_2^2 - c_1 - c_2}{2} \\
a(-2,0,0) &= -a(-1,0,0) - c_1c_2 + 1 \\
a(-2,0,1) &= -a(-1,0,1) + 2c_1c_2 \\
a(-2,0,2) &= -a(-1,0,2) - c_1c_2
\end{aligned} \tag{19}
$$

where

$$
\begin{aligned}
c_1 &= c/2\cos\phi_1 \\
c_2 &= c/2\cos\phi_2.
\end{aligned} \tag{20}
$$

The reflection function has been obtained for the Liao ABC using both the FDTD simulation and the numerical-calculation procedure for two configurations of the ABC with the variables c_1 and c_2 (20) being chosen to obtain theoretical angles of complete absorption as follows, where: a) $\phi_1 = \phi_2 = 0^\circ$ and b) $\phi_1 = 5^\circ$ and $\phi_2 = 30^\circ$.

Fig. 4 displays the results of these simulations. As can be seen from these results, the data obtained from the numerical formulation is indistinguishable from that obtained by FDTD simulation. It is also plainly obvious that the performance of this ABC is extremely poor. This is a direct consequence of having to interpolate the field values in space, thus limiting the accuracy of the ABC to that of the quadratic interpolation.

V. ABC Optimization

If the effects that the finite discretizations have upon the time-space ABC's are studied, one finds that as the mesh becomes coarser (decreasing $\lambda/\Delta z$), the ABC performance degrades [10]. This can be observed in Fig. 5, where the reflection from the second-order Higdon ABC (17) has been calculated for a number of mesh discretizations. One can see that as the mesh discretization ratio is increased ($\lambda/\Delta z \to \infty$) that the reflection function for this ABC approaches the optimal level of performance, displaying zeros for the desired angles of incidence. The object of this section is to show that one can solve for the various weighting parameters of all time-space ABC's such that the desired optimum performance can be achieved, regardless of the level of discretization of the FDTD mesh.

If one examines the equation which is used to calculate the reflection from an ABC (7), one can readily see that the numerator and denominator are effectively polynomials of the three variables $e^{j\omega\Delta t}$, $e^{-jk_x\Delta x}$, and $e^{jk_z\Delta z}$, where the $a(n,i,k)$ serve as the polynomial coefficients. Now the performance of the ABC (as previously defined) is measured only as a function of the incident angle; thus, $e^{j\omega\Delta t}$ remains constant. Since k_x is related to k_z by the dispersion relation, then one effectively have a polynomial of only a single variable $e^{-jk_z\Delta z}$. Because this reflection function is a polynomial, finding the incident angles where the reflection is zero is equivalent to finding the roots of the numerator. Conversely, the ABC may be designed to have zeros for certain angles of incidence simply by correctly setting the weighting parameters $a(n,i,k)$.

Upon forming an equation to calculate the reflection from an ABC, one can *sometimes* solve for the necessary weighting parameters $a(n,i,k)$ to obtain zero reflection at the required angles of incidence. For example, one may wish to achieve zero reflection from an ABC discretized in the form given by (8) for an incident wave with normal wavenumber component $k_1 = k\ \cos(\phi_1)$. To achieve $R_{\rm ABC} = 0$, one could solve for either $a(0,0,1)$, $a(-1,0,0)$, and $a(-1,0,1)$, or, to retain the nature of the ABC, one could solve for the parameter γ, as follows. Neglecting the denominator from (10), one obtains

$$R_{\rm ABC} = 0 = 1 - e^{-j\omega\Delta t + jk_1\Delta z} - \gamma e^{-j\omega\Delta t} + \gamma e^{+jk_1\Delta z} \tag{21}$$

where $k_1 = k\ \cos(\phi_1)$ and $\cos(\phi_1)$ is the angle of complete absorption. After some manipulation, one can then deduce the following:

$$\gamma = \frac{\sin\left(\frac{k_1\Delta z - \omega\Delta t}{2}\right)}{\sin\left(\frac{k_1\Delta z + \omega\Delta t}{2}\right)}. \tag{22}$$

The reflection function for this ABC can then be obtained by substituting (22) back into (10)

$$R_{\rm ABC} = -e^{+jk_z\Delta z}\frac{\sin\left(\frac{k_1 - k_z}{2}\right)}{\sin\left(\frac{k_1 + k_z}{2}\right)}. \tag{23}$$

By inspection, it can be seen that this function will have only one zero, and it will occur when the incident wavenumber (normal component) is $k_z = k_1$. This also identifies the ABC as first-order by definition.

If one applies Taylor expansions to the sine terms in (23), then to the leading order, this equation has the same form as the optimum-performance equation (2). This new formulation for the boundary condition will now be defined as being optimal, since it now perfectly absorbs at the required angle of incidence.

The method described above for optimizing the time-space boundary conditions, solving for $R_{\rm ABC} = 0$, has been applied to the three boundary conditions mentioned previously: the second-order ABC of Trefethen and Halpern, the second-order Higdon using the box-scheme discretization, and the second-order modified Liao ABC. For the second-order Trefethen and Halpern (14) and Higdon (17) boundary conditions, it was possible to retain the character of the boundary conditions and solve only for their governing variables p_0, p_2, γ_1, and γ_2. In the case of the modified Liao boundary condition (19), this was not possible, and the ABC weightings $a(n,i,k)$ were solved for instead. The results of these optimizations are as follows.

Trefethen and Halpern's Second-Order ABC:

$$\begin{aligned} p_0 &= \frac{c^2 + a_1}{ca_2} \\ p_2 &= -\frac{a_1}{ca_2} \end{aligned} \tag{24}$$

where c is the speed of light and

$$\begin{aligned} a_1 &= \frac{\Delta z^2 \sin^2\left(\frac{\omega\Delta t}{2}\right)}{\Delta t^2 \sin\left(\frac{k_1\Delta z}{2}\right)\sin\left(\frac{k_2\Delta z}{2}\right)\cos\left(\frac{k_1\Delta z + k_2\Delta z}{2}\right)} \\ a_2 &= \frac{\Delta z \sin\left(\frac{\omega\Delta t}{2}\right)\cos\left(\frac{k_1\Delta z}{2}\right)\cos\left(\frac{k_2\Delta z}{2}\right)\sin\left(\frac{k_1\Delta z + k_2\Delta z}{2}\right)}{\Delta t \cos\left(\frac{\omega\Delta t}{2}\right)\sin\left(\frac{k_1\Delta z}{2}\right)\sin\left(\frac{k_2\Delta z}{2}\right)\cos\left(\frac{k_1\Delta z + k_2\Delta z}{2}\right)}. \end{aligned} \tag{25}$$

Higdon's Second-Order ABC:

$$\gamma_i = \frac{\sin\left(\frac{k_i\Delta z - \omega\Delta t}{2}\right)}{\sin\left(\frac{k_i\Delta z + \omega\Delta t}{2}\right)}. \tag{26}$$

The Second-Order Modified Liao ABC:

$$\begin{aligned} a(-1,0,0) &= 2\cos(\omega\Delta t) - \sin(\omega\Delta t) \\ &\quad \cdot \left(\frac{\cos(k_1\Delta z)}{\sin(k_1\Delta z)} + \frac{\cos(k_2\Delta z)}{\sin(k_2\Delta z)}\right) \\ a(-1,0,1) &= \sin(\omega\Delta t)\left(\frac{1}{\sin(k_1\Delta z)} + \frac{1}{\sin(k_2\Delta z)}\right) \\ a(-1,0,2) &= 0 \\ a(-2,0,0) &= \cos(\omega\Delta t)\sin(\omega\Delta t) \\ &\quad \cdot \left(\frac{\cos(k_1\Delta z)}{\sin(k_1\Delta z)} + \frac{\cos(k_2\Delta z)}{\sin(k_2\Delta z)}\right) - \cos^2(\omega\Delta t) \\ &\quad - \sin^2(\omega\Delta t)\frac{\cos(k_1\Delta z)\cos(k_2\Delta z)}{\sin(k_1\Delta z)\sin(k_2\Delta z)} \\ a(-2,0,1) &= \frac{\sin^2(\omega\Delta t)}{\sin(k_1\Delta z)\sin(k_2\Delta z)} \\ &\quad \cdot (\cos(k_1\Delta z) + \cos(k_2\Delta z)) - \cos(\omega\Delta t) \\ &\quad \cdot \sin(\omega\Delta t)\left(\frac{1}{\sin(k_1\Delta z)} + \frac{1}{\sin(k_2\Delta z)}\right) \\ a(-2,0,2) &= -\frac{\sin^2(\omega\Delta t)}{\sin(k_1\Delta z)\sin(k_2\Delta z)}. \end{aligned} \tag{27}$$

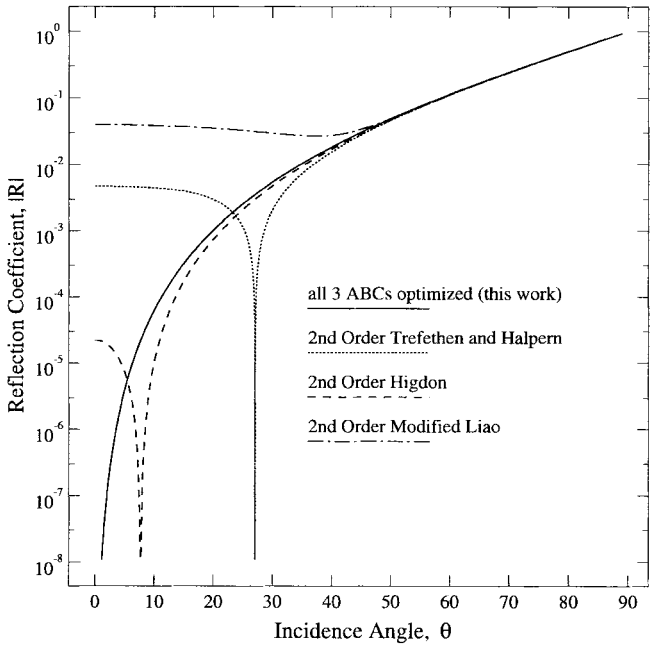

Fig. 6. Reflection coefficients from both the standard and optimized second-order ABC's as a function of incidence angle $\lambda/\Delta z = 20$. Designated angles of complete absorption are $\phi_1 = \phi_2 = 0°$.

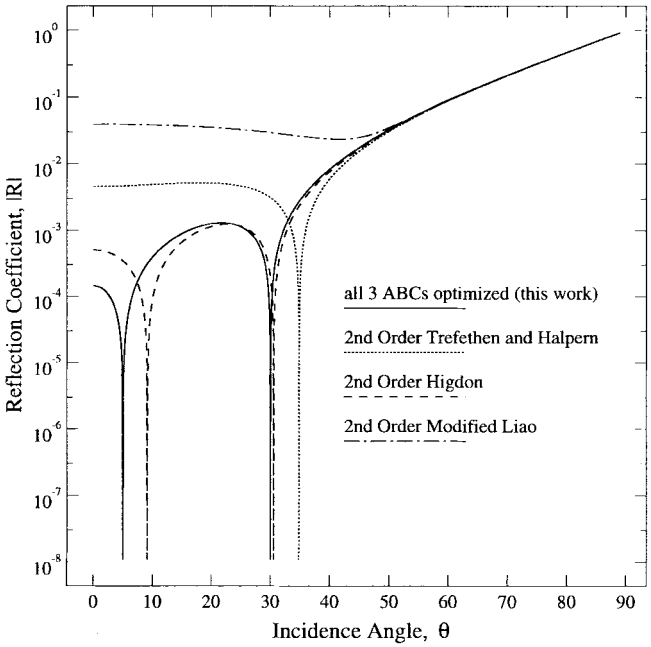

Fig. 7. Reflection coefficients from both the standard and optimized second-order ABC's as a function of incidence angle $\lambda/\Delta z = 20$. Designated angles of complete absorption are $\phi_1 = 5°$ and $\phi_2 = 30°$.

An interesting point to note is that when the assumptions $|k_z \Delta z| \ll 1$ and $|\omega \Delta t| \ll 1$ are made, the parameters given above for the ABC of Trefethen and Halpern, and that by Higdon, (24) and (26), can be reduced to those designed for the original boundary conditions (16) and (18).

The reflection functions are calculated for the above optimized boundary conditions using the calculation procedure described earlier, with the mesh-discretization parameter set to 20 cells per wavelength $(\lambda/\Delta z = 20)$. The reflection functions for the three ABC's in their standard original form are then compared to the results achieved for the optimized ABC's. Since the reflection functions for all three of the optimized ABC's are indistinguishable, only one set of results will be displayed.

Fig. 6 shows the reflection function for all three ABC's when they are designed for absorption at normal incidence $\phi_1 = \phi_2 = 0°$. It can be clearly seen that these ABC's perform poorly when applied in their original form, yet when these ABC's are optimized they all converge upon the same optimum level of absorption.

Fig. 7 shows the reflection function for the ABC's when they are designed for perfect absorption at two angles—$\phi_1 = 5°$ and $\phi_2 = 30°$. Again, the improvement which can be obtained is obvious.

Fig. 8 shows the reflection function resulting from the analysis of the optimized second-order Higdon ABC for a coarse and a fine mesh. Compared to the optimal reflection function, one can observe that the zeros of the reflection functions for both coarse- and fine-mesh simulations are at the desired positions. However, one can also see that away from the zeros, the reflection by the ABC's is slightly greater than that predicted by the optimal reflection function (2). This is expected as the optimal reflection function is an approximation

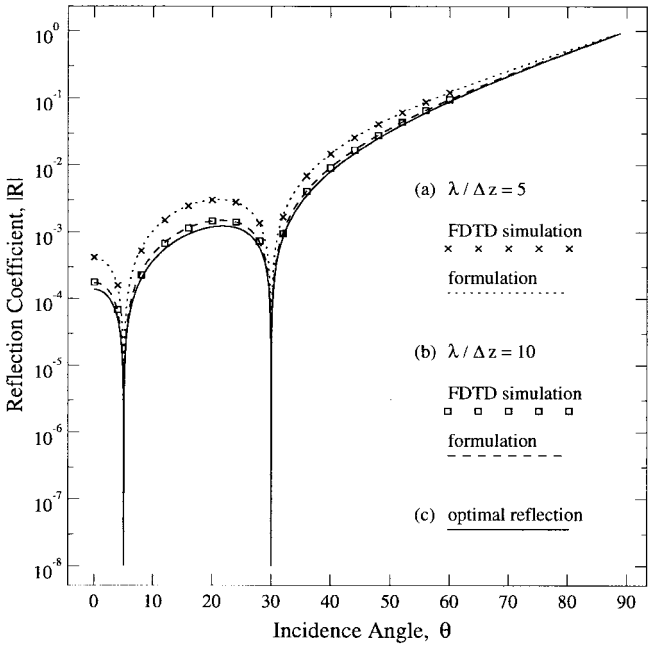

Fig. 8. The reflection function obtained by formulation and FDTD simulation for an optimized second-order Higdon ABC with complete absorption at $\phi_1 = 5°$ and $\phi_2 = 30°$. (a) $\lambda/\Delta z = 5$, (b) $\lambda/\Delta z = 10$, and (c) the optimal reflection function (2).

and will become less accurate as the mesh resolution decreases. Compared to the results achieved by FDTD simulation, one can again see that the formulation method is very accurate.

Another form of the boundary-truncation technique, which has appeared often in the literature, is the superabsorbing-boundary algorithm proposed by Fang and Mei [7]—a method which is applied in conjunction with other time-space ABC's to improve their level of absorption. While not exactly being

a time-space boundary condition by definition, it is worthy of consideration by the optimization procedure outlined above.

The basis of the super-absorption technique revolves around performing the chosen time-space absorbing-boundary condition (e.g., first-order Mur) twice, once at the boundary and once at half a spatial increment inside the mesh, half a time step later. The superabsorbing-boundary algorithm is then employed to increase the accuracy of the boundary truncation by using the error created by the calculation of the outer boundary to cancel the error produced by the calculation of the inner boundary.

It has been shown that the total reflection from the mesh boundary is the product of the reflection from the time-space ABC and the reflection resulting from the superabsorbing-boundary algorithm [18, p. 1003]. Thus, one only needs to be concerned with optimizing the superabsorbing-boundary algorithm. To do this, one can solve for $R_{\text{superabsorber}}(\rho) = 0$, where ρ is a variable that is used to define the angle at which the algorithm best performs the error correction. The following is achieved for an optimal solution:

$$\rho = \frac{\sin\left(\frac{\omega\Delta t}{2}\right)}{\sin\left(\frac{k_1\Delta z}{2}\right)}\, e^{-j\left(\frac{\omega\Delta t + k_1\Delta z}{2}\right)}. \tag{28}$$

To demonstrate the absorption improvement achieved by applying the superabsorbing-boundary algorithm, three analyses have been performed. The first-order ABC (8) has first been implemented at the boundary with the variable γ (22), chosen such that the theoretical angle of complete absorption is $\phi_1 = 5°$. Next, the analysis has been repeated with the superabsorbing-boundary algorithm applied in its original form with $\rho = c\Delta t/\Delta z \cos(\phi_2)$, where $\phi_2 = 30°$. Finally, the analysis has been performed with the optimal choice for ρ (28).

Fig. 9 displays the results of these simulations. One can see that the absorption abilities of the optimized first-order ABC have been improved by applying the superabsorbing-boundary algorithm. The improvement does not appear to be as good as that obtained simply by implementing a second-order Higdon ABC (see Fig. 3). It can also be seen that no extra zeros have appeared within the reflection function even though the superabsorbing-boundary algorithm has been tailored for perfect absorption at $\phi_2 = 30°$. However, once the superabsorbing algorithm has been optimized, one can see the appearance of the second zero and the obvious improvement in the reflective properties. This result, achieved for the optimized superabsorbing algorithm and applied with an optimized first-order ABC, is equivalent to that achieved for all of the optimized second-order boundaries (see Fig. 7). This suggests that implementation of the superabsorbing-boundary algorithm, to improve the absorptive abilities of a time-space ABC, effectively increases the order of that time-space ABC by one.

It should be noted that this variable ρ is complex, and as a result, the superabsorbing-boundary algorithm can only perform optimally in a mesh which is computed using complex numbers.

It is quite clear from the results presented that all of these boundary conditions are able to achieve the optimal level of performance and that the only difference between them are their methods of implementation. However, when considering the use of higher order boundary conditions, the Higdon formulation is the best of these time-space-type absorbing boundaries as a result of its simple mathematical construction and the ease by which it can be optimized by choosing the parameter γ (26).

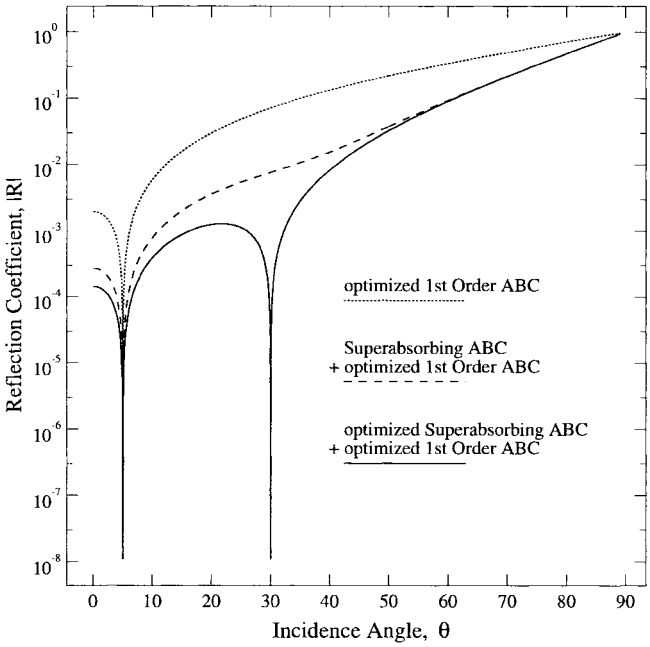

Fig. 9. The reflection function for an optimized first-order ABC with complete absorption at $\phi_1 = 5°$, $\lambda/\Delta z = 20$. (a) Without the superabsorbing-boundary algorithm, (b) with the superabsorbing-boundary algorithm, and (c) with the optimized superabsorbing-boundary algorithm. $\phi_2 = 30°$.

VI. Conclusion

A general numerical method has been demonstrated, which enables the calculation of the reflection properties of time-space ABC's. The accuracy of this method has been proven by comparison with data obtained by FDTD simulation for a number of commonly used time-space ABC's.

A criterion for the classification of time-space ABC's has been defined and an optimal absorbency has been described for ABC's of a given order. It has been demonstrated, by correct choice of parameters, that this optimal level of absorption can be achieved by all boundary conditions of the type described, regardless of the mesh discretization. The reflective equivalence between the second-order ABC of Trefethen and Halpern, the second-order Higdon (box-scheme discretization), Fang and Mei's superabsorbing-boundary algorithm applied with a first-order ABC, and the second-order modified Liao ABC's has also been demonstrated.

Acknowledgment

The authors would like to acknowledge the reviewers for their helpful comments and constructive criticisms that led to a substantial improvement of this paper.

REFERENCES

[1] G. Mur, "Absorbing boundary conditions for the finite-difference approximation of the time-domain electromagnetic-field equations," *IEEE Trans. Electromag. Compat.*, vol. EMC-23, pp. 377–382, Nov. 1981.

[2] L. N. Trefethen and L. Halpern, "Well-posedness of one-way wave equations and absorbing boundary conditions," *Math. Comput.*, vol. 47, no. 176, pp. 421–435, Oct. 1986.

[3] R. L. Higdon, "Absorbing boundary conditions for difference approximations to the multi-dimensional wave equation," *Math. Comput.*, vol. 47, no. 176, pp. 437–459, Oct. 1986.

[4] Z. P. Liao, H. L. Wong, Y. Baipo, and Y. Yifan, "A transmitting boundary for transient wave analyzes," *Scientia Sinica*, (Series A), vol. 27, no. 10, pp. 1062–1076, Oct. 1984.

[5] J. G. Blaschak and G. A. Kriegsmann, "A comparative study of absorbing boundary conditions," *J. Comput. Phys.*, vol. 77, pp. 109–139, 1988.

[6] R. H. Feng, P. S. Koopi, M. S. Leong, T. S. Yeo, and P. J. Hum, "Efficiencies of the Liao's and Mur's absorbing boundary conditions," in *Asia–Pacific Microwave Conf. Dig.*, Tokyo, Japan, Dec. 1994, pp. 991–994.

[7] J. Fang and K. K. Mei, "A super-absorbing boundary algorithm for solving electromagnetic problems by time-domain finite-difference method," in *IEEE AP-S Int. Symp. Dig.*, Syracuse, NY, June 1988, pp. 472–475.

[8] Z. Bi, K. Wu, and J. Litva, "Designing dispersive boundary condition (DBC) for the FD-TD method using digital filtering theory," in *IEEE AP-S Int. Symp. Dig.*, Chicago, IL, July 1992, pp. 326–329.

[9] C. J. Railton, E. M. Daniel, D. L. Paul, and J. P. McGeehan, "Optimized absorbing boundary conditions for the analysis of planar circuits using the finite difference time domain method," *IEEE Trans. Microwave Theory Tech.*, vol. 41, pp. 290–297, Feb. 1993.

[10] C. J. Railton and E. M. Daniel, "Comparison of the effect of discretization on absorbing boundary algorithms in the finite difference time domain method," *Electron. Lett.*, vol. 28, no. 20, pp. 1891–1893, Sept. 24, 1992.

[11] W. C. Chew and R. L. Wagner, "A modified form of Liao's absorbing boundary condition," in *IEEE AP-S Int. Symp. Dig.*, Chicago, IL, July 1992, pp. 536–539.

[12] A. Taflove and K. R. Umashankar, "The finite-difference time-domain method for numerical modeling of electromagnetic wave interactions," *Electromagnetics*, vol. 10, pp. 105–126, 1990.

[13] R. L. Higdon, "Numerical absorbing boundary conditions for the wave equation," *Math. Comput.*, vol. 49, no. 179, pp. 65–90, July 1987.

[14] J. Fang, "Absorbing boundary conditions applied to model wave propagation in microwave integrated-circuits," *IEEE Trans. Microwave Theory Tech.*, vol. 42, pp. 1506–1513, Aug. 1994.

[15] L. A. Vielva, J. A. Pereda, A. Vegas, and A. Prieto, "Simulating 3-D waveguide discontinuities using a combination of Prony's method and FDTD with improved absorbing boundary conditions," *IEE Proc. Microwave Antennas Propagat.*, vol. 141, no. 2, pp. 127–132, Apr. 1994.

[16] Z. Bi, K. Wu, C. Wu, and J. Litva, "A dispersive boundary condition for microstrip component analysis using the FD-TD method," *IEEE Trans. Microwave Theory Tech.*, vol. 40, pp. 774–777, Apr. 1992.

[17] D. T. Prescott and N. V. Shuley, "Reducing solution time in monochromatic FDTD waveguide simulations," *IEEE Trans. Microwave Theory Tech.*, vol. 42, pp. 1582–1584, Aug. 1994.

[18] K. K. Mei and J. Fang, "Superabsorption—A method to improve absorbing boundary conditions," *IEEE Trans. Antennas Propagat.*, vol. 40, pp. 1001–1010, Sept. 1992.

Deane T. Prescott (S'91–M'97) was born in Auckland, New Zealand, on January 11, 1969. He received the B.E. and Ph.D. degrees in electrical engineering from the University of Queensland, Queensland, Australia, in 1990 and 1996, respectively.

Since April 1996, he has been working at the Australian Defense Science and Technology Organization (DSTO), Salisbury, Australia, where he is involved with the measurement and numerical prediction of the RCS of aerial targets. His research interests include the development and application of numerical techniques such as the FDTD method, absorbing boundary conditions, frequency-selective surfaces, and RCS prediction.

Nicholas V. Shuley (S'79–M'85) was born in Melbourne, Australia, in April 1951. He received the B.E. and M.Eng.Sc. degrees from the University of New South Wales, Australia, in 1973 and 1975, respectively, and the Ph.D. degree in electrical engineering from Chalmers University of Technology, Gothenburg, Sweden, in 1985.

From 1977 to 1978, he was with Microwave Associates, Dunstable, U.K., where he was concerned with the design and development of microwave solid-state circuit power generation. From 1979 to 1988, he was a Research and Teaching Assistant and, later, a Post-Doctoral Scientist with the Division of Network Theory at Chalmers University of Technology, Gothenburg, Sweden. During 1996, he was a Visiting Scientist with the Department of Electronics and Electromagnetics within the Department of Physics at the University of Seville, Seville, Spain. He is currently with the Department of Electrical and Computer Engineering at the University of Queensland, Queensland, Australia, where he is supervising research in computational electromagnetics and electromagnetic modeling of dichroic surfaces and microwave antennas. He has also done consulting work for the European Space Agency.

Dr. Shuley has been a member of the Microwave Theory and Techniques Editorial Board since 1992, and shared the Best Paper Award at JINA 1988.